PII: S0032-3861(96)00776-8

Polymer Vol. 38 No. 9, pp. 2057–2065, 1997

0032-3861/97/$17.00+0.00

Proton transport in polyacrylamide based hydrogels doped with H_3PO_4 or H_2SO_4

W. Wieczorek and J. R. Stevens*
Department of Physics, University of Guelph, Guelph, Ontario, Canada N1G 2W1
(Received 2 April 1996; revised 17 July 1996)

Protonic transport in polyacrylamide hydrogels doped with H_3PO_4 or H_2SO_4 has been studied using impedance spectroscopy, Fourier transform infra-red (*FT* i.r.) and differential scanning calorimetry (d.s.c.) techniques. These hydrogels exhibit room temperature conductivities greater than 10^{-2} S cm^{-1}; these increase with temperature to 10^{-1} S cm^{-1} at 100°C. D.s.c. experiments show that H_3PC_4 doped hydrogels do not undergo any first-order transitions up to 100°C whereas hydrogels doped with H_2SO_4 decompose at temperatures higher than 70°C. It is shown from conductivity and *FT* i.r. studies that the concentration of acids and the concentration of water influence the proton transport mechanisms. Long-time conductivity studies performed at temperatures between 70 and 100°C indicate 'drying' of hydrogels, which results in a decrease in conductivity; conductivities remain stable below 70°C. © 1997 Elsevier Science Ltd.

(Keywords: H_3PO_4; hydrogels; conductivity)

INTRODUCTION

Polymer solid electrolytes form an interesting group of ionically conductive materials which combine properties characteristic of solid and liquid electrolytes. This feature results in a variety of possible applications of ionically conductive polymers in various electrochemical devices working in a wide temperature range, e.g. −50 to 150°C. Some examples of these devices are alkali metal batteries, electrochromic displays, sensors and fuel cells. Recent developments in the application of polymeric electrolytes have been reviewed by Scrosati[1]. Most alkali metal conducting systems have been studied in the solid state form or as highly conductive gels in which low molecular weight solvents are trapped inside a polymer host[1].

The development of novel proton conducting polymeric electrolytes for various electrochemical applications has attracted attention, as reviewed by Lassegues[2]. The systems described are polymers having Lewis base centres in their structure, e.g. polyamides[2,3], polyimines[2,4] or polyethers[2,5] doped with strong inorganic acids such as H_2SO_4 or H_3PO_4. For these systems the mechanism of proton conduction has been inferred from conductivity, Fourier transform infra-red (*FT* i.r.) and nuclear magnetic resonance (n.m.r.) data[2–5].

According to literature indications[2,3] 'dry' complexes of linear polyacrylamide (PAAM) and strong inorganic acids, such as H_3PO_4 or H_2SO_4, exhibit the highest ambient temperature protonic conductivities; these are in the range 5×10^{-4}–5×10^{-3} S cm^{-1}. Conductivity increases with temperature to about 10^{-2} S cm^{-1} at 100°C. However, the mechanical and chemical stability of protonic electrolytes based on linear polymers is poor and degradation is often observed after humidification. On the other hand, it is possible to obtain hydrogels in the form of thin films of reasonable mechanical strength. This can be achieved by the preparation of composite interpenetrating network hydrogels. These hydrogels can be obtained by the copolymerization of acrylamide with *N,N'*-methylenebisacrylamide (MBAA) in aqueous solution with some natural polymers (e.g. agar) which can form three-dimensional networks[6,7].

Preliminary studies on PAAM based hydrogels doped with H_3PO_4[8] and H_2SO_4[9] have been performed. It has been shown that the conductivity of hydrogels depends on the concentration of acid, water and cross-linking and gelation agents. Room temperature conductivities up to 2×10^{-2} S cm^{-1} were measured for H_3PO_4 doped electrolytes; conductivities increase with an increase in temperature up to 10^{-1} S cm^{-1} at 100°C. Hydrogels doped with H_2SO_4 exhibit similar ambient temperature conductivities to those obtained for the same polymers doped with H_3PO_4. However, for gels containing a high concentration of H_2SO_4 a decrease in conductivity was observed at temperatures exceeding 60°C. This decrease results from dehydration of the hydrogels or from degradation of the polymer matrix; both occur in the presence of a strong inorganic acid. Such a tendency has not been observed for the systems doped with H_3PO_4.

The main goal of this report is to discuss our study of the relationship between the conductivity and structure of hydrogel electrolytes relying on data from impedance spectroscopy, *FT* i.r. and differential scanning calorimeters (d.s.c.). The long term stability of the conductivity of hydrogels is also studied in the temperature range 70–100°C. In order to explain proton conduction in hydrogels a comparison is made between the 'dry' systems studied by Lassegues *et al.*[2,3] and hydrogel electrolytes. The ionic conductivity of hydrogels is analysed as a function of water concentration and temperature using an effective medium theory (EMT) approach.

* To whom correspondence should be addressed

EXPERIMENTAL

Sample preparation

Proton conducting gel electrolytes were prepared according to the following procedure. Acrylamide (AAM) (Eastman Kodak, reagent grade), MBAA (Aldrich, reagent grade) and agar (Aldrich, reagent grade) were mixed together in a glass flask and dissolved in deionized water. Stirring was continued until there was visible dissolution of the solid components. This was followed by the addition of stoichiometric amounts of H_3PO_4 in the form of 85 wt% aqueous solution (Fischer Scientific, reagent grade). The H_3PO_4 concentration in the electrolytes has been calculated as an H_3PO_4/AAM molar ratio and was varied in the range 1/1–2/1. After about 30 min of mixing, a few drops of H_2O_2 (acting as an initiator for the polymerization reaction) was added. The reaction mixture was placed in an oven at 75–80°C for *ca* 80 min. After this time the gelation process was observed and the temperature was then reduced to 60°C. The samples were kept at this temperature for approximately a further 1 h.

In a variation of the above (primary) procedure, H_3PO_4 was added just after the first traces of gelation were observed. However, in this procedure it is difficult to ascertain when gelation begins; uncertainty here usually leads to non-reproducible products.

We have also tried to prepare proton conducting gels by the synthesis of an undoped gel (i.e. no H_3PO_4) according to the procedure described above. The gels were then soaked in an aqueous solution of H_3PO_4. The quality of gels obtained was similar to that observed for gels prepared by our primary procedure. However, it was usually difficult to assure complete incorporation of the acid by the gel. Therefore, most of the samples studied were prepared by our primary procedure. The amount of water included in the gel was calculated on the basis of gravimetric measurements.

Proton conducting hydrogels doped with H_2SO_4 were also prepared according to the primary procedure; H_2SO_4 was used in the form of a 50 wt% aqueous solution. It was found necessary to reduce the reaction temperature to 70°C (5–10°C lower than for the gels doped with H_3PO_4). The gelation process started to occur after *ca* 35 min of the reaction. The temperature was then reduced to approximately 60°C, and the samples were kept at this temperature for approximately a further 30 min. The H_2SO_4/AAM molar ratio was varied between 1/1 and 2/1. The water content was approximately 30–35 wt% for all the samples studied. The composition of the gel protonic electrolytes synthesized is summarized in *Table 1*. For the purposes of the EMT calculations the volume fraction of water has been estimated on the basis of the known specific gravities of PAAM, H_3PO_4 and water. The additiveness of volume fractions of all components was assumed.

EXPERIMENTAL TECHNIQUES

D.s.c. studies

D.s.c. data were obtained between −110 and 150°C using a Dupont TA 2910 scanning calorimeter with a low temperature measuring head and a liquid nitrogen-cooled heating element. Samples (approximately 15 mg) were loaded into aluminium pans and then stabilized by slow cooling from room temperature to −110°C. Samples were then heated at 10°C min^{-1} to 150°C (Run I). Immediately following Run I a second 'Run II' was started in which samples were slowly cooled from 150 to −110°C and then heated to 150°C. An empty aluminium pan was used as a reference.

Conductivity measurements

Ionic conductivity was determined using the complex impedance method. The samples were sandwiched between two stainless steel blocking electrodes, sealed in a quartz tube and placed in a temperature controlled furnace. The impedance measurements were carried out on a computer-interfaced HP 4192A impedance analyser over the frequency range 5Hz–13 MHz. The peak-to-peak voltage was 1 V. Typical impedance spectra (Nyquist plots, drawn on a complex plane) consist of a high frequency distorted semicircle and a low frequency spike. The high frequency semicircle represents bulk relaxation phenomena in these hydrogel electrolytes whereas the low frequency spike is related to electrode/electrolyte interfacial phenomena. Bulk ionic d.c. resistances (R_b) of these electrolytes were calculated as an arithmetic mean of the two values obtained, respectively, from the intersection of the spike with the real impedance axis and the intersection of the low frequency end of the semicircle with the same axis. With an increase in temperature both of the above intersections shift to

Table 1 Composition of hydrogel electrolytes and T_g values obtained from d.s.c. experiments

Sample code	Mass of MBAA (g)	Mass of agar (g)	Acid used	Acid/AAM molar ratio	T_g (Run I) (°C)	T_g (Run II) (°C)
1	0.030	0.304	H_3PO_4	1.6	−76	−75
2	0.057	0.102	H_3PO_4	1.6	−78	−55
3	0.030	0.203	H_3PO_4	1.6	−81	−49
4	0.059	0.300	H_3PO_4	1.6	−85	−70
5	0.092	0.302	H_3PO_4	1.6	−60	−57
6	0.030	0.302	H_2SO_4	1.0	−60	−48
7	0.029	0.304	H_2SO_4	1.2	−78	−57
8	0.031	0.299	H_2SO_4	1.4	−66	−59
9	0.030	0.298	H_2SO_4	1.6		
10	0.029	0.301	H_2SO_4	1.8	−57	
11	0.030	0.300	H_2SO_4	2.0	−17	

higher frequencies. Knowing R_b, the ionic conductivity of the hydrogel electrolyte (σ) can be calculated as $\sigma = l/(AR_b)$. Here, l is the thickness of the electrolyte under measurement, and A is the geometrical area of each electrode.

FT*i.r. studies*

I.r. spectra were recorded on a computer interfaced Nicolet *FT* i.r. system 4.4 instrument with a wavenumber resolution of $2\,cm^{-1}$ in the range $4000–400\,cm^{-1}$. Thin film electrolyte foils were sandwiched between two NaCl plates.

RESULTS AND DISCUSSION

Conductivity studies—effect of water and H_3PO_4 concentration

Figure 1 depicts the variation of the room temperature (RT) ionic conductivity of polymeric gels *versus* the concentration of acids (H_2SO_4 and H_3PO_4) (denoted as acid/AAM molar ratio). For H_3PO_4 doped hydrogels, conductivity increases from 10^{-3} $S\,cm^{-1}$ (H_3PO_4/AAM = 1.2) to $2 \times 10^{-2}\,cm^{-1}$ (H_3PO_4/AAM = 1.6) and remains almost constant for higher concentrations of H_3PO_4. Similar to that for the H_3PO_4 doped electrolytes the conductivity for H_2PO_4 doped hydrogels increases from 3.8×10^{-4} $S\,cm^{-1}$ (H_2SO_4/AAM = 1 : 1) to 1.7×10^{-2} $S\,cm^{-1}$ (H_2SO_4/AAM = 1.6 : 1) and remains almost constant for higher concentrations of H_2SO_4. The variation of the RT conductivity with the acid/AAM ratio is similar to that obtained by Lassegues *et al.*[2,3] for PAAM/H_2SO_4 and PAAM/H_3PO_4 protonic solid electrolytes. However, conductivities measured for hydrogels are about one order of magnitude higher. Lassegues *et al.* based the conductivity behaviour observed on the protonation of polymer Lewis base sites by acid molecules. According to their assumptions[2,3] at acid/PAAM ratios higher than 1 complete protonation occurs and the density of HSO_4^- anions was high enough to create a conduction path. In partially protonated systems the dominant interactions are intra- and/or inter-chain hydrogen bonds between protonated and non-protonated Lewis base sites. Conduction should occur by proton exchange between these sites. For acid concentrations for which the conductivity reaches a plateau, conduction seems to be dominated by the self-ionization of excess acid. Also, conductivity can occur via an exchange of protons between protonated amid resonance forms[2]. In the case of hydrogels the effect of water must be considered since, as has been pointed out above, the presence of water facilitates ionic transport and enhances the conductivity.

Figure 2 shows changes in the RT ionic conductivity of a gel protonic electrolyte (H_3PO_4/AAM ratio equal to 1.6/1) as a function of water concentration. The conductivity increases with an increase in water concentration up to about 40–45 vol% and then remains almost constant up to 70 vol%. Between 45 and 70 vol% of water RT conductivities exceeded $10^{-2}\,S\,cm^{-1}$.

In *Figure 3* changes of conductivity *versus* reciprocal temperature are shown for samples of a H_3PO_4/AAM molar ratio equal to 1.6/1 containing, respectively, 11 vol% of water (*Figure 3a*) and 70 vol% of water (*Figure 3b*). For water concentrations exceeding 45 vol% the temperature dependence of conductivity is of the Arrhenius form:

$$\sigma = \sigma_0 \exp\frac{-E_a}{k_B T} \quad (1)$$

Here, E_a is the activation energy for conduction, σ_0 is a pre-exponential factor, and k_B is the Boltzmann constant.

In our opinion this results from the fact that, for higher water concentrations, ionic conductivity occurs via interstitial water pathways present in the polymer matrix. The relatively constant ionic conductivity as a function of the concentration of water confirms such an hypothesis.

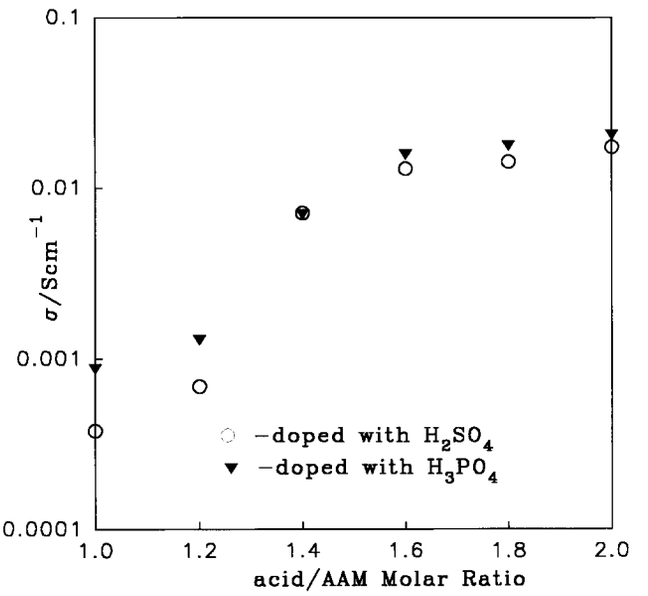

Figure 1 Dependence of the room temperature ionic conductivity of PAAM based protonic gel electrolytes on the acid/AAM molar ratio concentration of H_3PO_4 or H_2SO_4. Samples contain 40 vol% of water

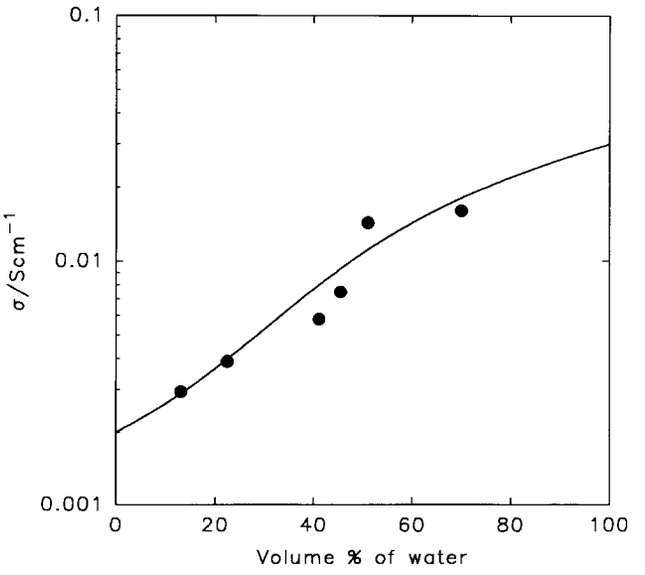

Figure 2 Ionic conductivity *versus* water concentration (w, in vol%) in a PAAM based protonic electrolyte (H_3PO_4/AAM = 1.6/1) at 25°C: (●) experimental data; (solid line) model data calculated on the basis of the EMT approach [equation (4)]

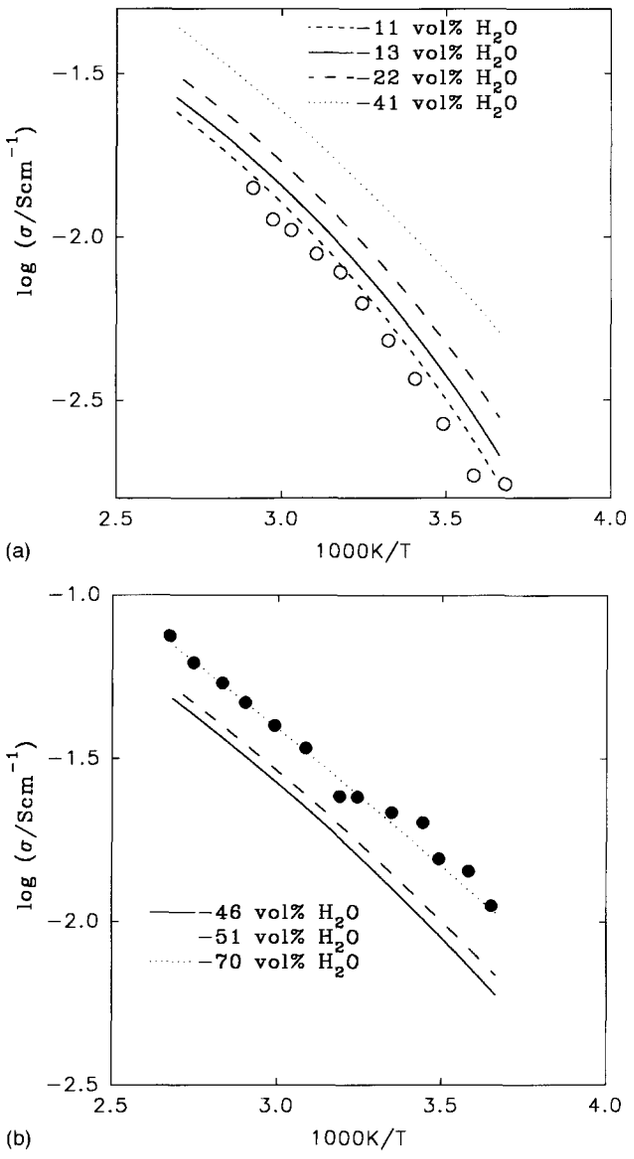

Figure 3 Ionic conductivity *versus* reciprocal temperature for PAAM based protonic gel electrolytes containing various amounts of water (H_3PO_4/AAM = 1.6/1). Solid, dashed or dotted lines show model data calculated on the basis of the EMT approach. Model data calculated for samples of various concentrations. Experimental data for samples containing: (a) (○) 11 vol% of water; (b) (●) 70 vol% of water

For lower water concentrations the temperature dependence of conductivity can be described by the VTF form [see equation (2)]; this is the same form as for 'dry' PAAM/H_3PO_4 electrolytes[2,3].

$$\sigma = \frac{A}{T^{\frac{1}{2}}} \exp - \frac{B}{k_B(T - T_0)} \qquad (2)$$

Here, A is a pre-exponential factor, B is the pseudoactivation energy, and T_0 is the thermodynamic glass transition temperature, which is usually 30–50 K lower than the glass transition temperature T_g, as measured by d.s.c. experiments.

D.s.c. studies

Figures 4a and *4b* show d.s.c. curves recorded for the H_3PO_4 and H_2SO_4 doped electrolytes, respectively. For the H_3PO_4 doped hydrogel no first-order transitions are observed up to about 100°C. The endothermic peak with a maximum observed at about 130°C can be attributed to the reaction of H_3PO_4 with itself, leading to the formation of polyacids. D.s.c. glass transition temperatures (T_g) are included in *Table 1* where it can be seen that 'Run II' values are usually much higher than those obtained in 'Run I'. This probably results from the evaporation of water during heating above 100°C in 'Run I'. Water molecules act as traces of plasticizer for the polymeric host and hence a decrease in the water concentration should lead to stiffening of the polymer host and an increase in T_g. The d.s.c. curve obtained for the hydrogel doped with H_2SO_4 is shown in *Figure 4b*. A broad exothermic transition beginning at about 65–70°C is observed. This can be associated with the degradation of the polymer matrix. The T_g values are not easy to identify. Similar to those for the hydrogels doped with H_3PO_4, T_g values measured in 'Run II' are higher than those obtained in 'Run I' experiments.

For H_3PO_4 based electrolytes the effect of MBAA and agar on the thermal properties of hydrogels is also studied. As can be seen in *Table 1*, T_g increases with an increase in the concentration of MBAA, which acts as a cross-linking agent (see samples 1, 4 and 5 in 'Run II'). A decrease in T_g with an increase in the amount of agar is also observed (compare samples 1 with 3 or 2 with 4). It seems that agar, acting as the gelation agent, absorbs water, which in turn plasticizes the gel.

FTi.r. studies of H_3PO_4 doped hydrogel electrolytes

Two regions of *FT*i.r. spectra (3500–2400 and 1300–800 cm^{-1}) are of particular interest[3,10–13]. The first region corresponds to the symmetric stretch N–H vibrations of the NH_2 amide groups (3500–3200 cm^{-1}) and the N–H symmetric stretch vibrations of protonated NH_3^+ groups (2800–2400 cm^{-1})[3,13]. All *FT*i.r. spectra obtained are characterized by broad peaks in these frequency ranges, which makes it difficult to perform any quantitative analysis. Qualitatively, these spectra confirm that both protonated and unprotonated NH_2 amide groups coexist for all of the samples studied. This implies that the transport of protons could occur via proton exchange between the unprotonated NH_2 and the protonated NH_3^+ groups.

The 1300–800 cm^{-1} i.r. region in which vibrations involving the presence of H_3PO_4 occur is easier to analyse, and information concerning, hydrogel microstructure and ionic equilibria can be obtained. The positions of the P=O and P–O–(R) (R = H or organic substituent) stretching modes depend on the symmetry of the system studied[11] and can be influenced by the bonding of the H_3PO_4 to the polymer chain. The positions of these bands can be described by the following empirical relations developed by Thomas and Chittenden[12]:

$$\nu_{P=O} = 930 + 40 \sum \prod i = 1260 - 1115\,cm^{-1} \qquad (3a)$$

$$\nu_{P-O(R)} = 650 + 40 \sum \prod i = 1030 - 900\,cm^{-1} \qquad (3b)$$

Here, $\prod i$ are empirical coefficients which describe the influence of the substitution of the hydrogen in the P–OH on the position of the band maxima. Note that the slopes in equations (3a) and (3b), calculated on the basis of experimental data (see *Table 2*), are similar for various hydrogel electrolytes studied and are equal to 8.0–8.5.

It is found that the different levels of H_3PO_4

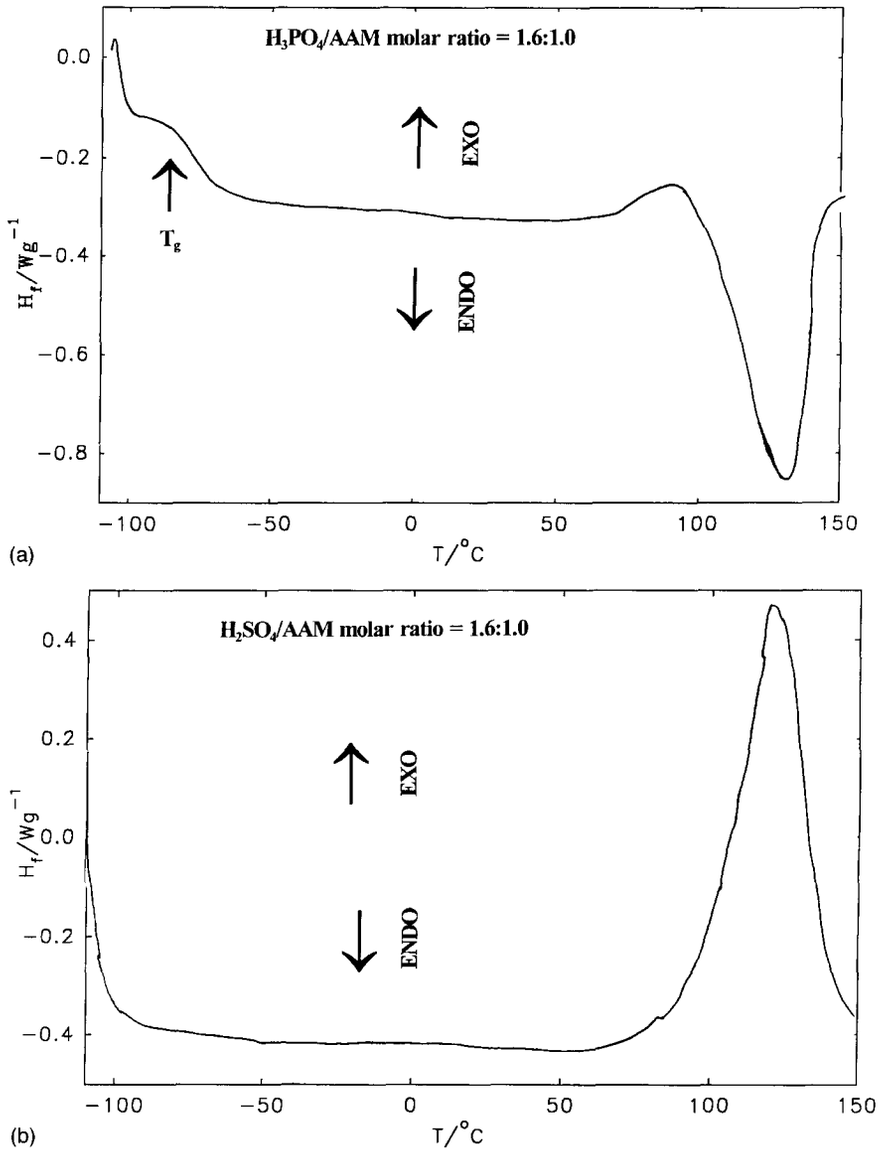

Figure 4 D.s.c. curves registered for hydrogel electrolytes doped with: (a) H_3PO_4; (b) H_2SO_4

dissociation and the interaction of H_3PO_4 with the polymer chain may influence the positions of the P=O and P–O–(R) bands. The P=O symmetric stretch band appears at approximately 1260 cm^{-1} and can be shifted down in frequency by up to 50–80 cm^{-1} due to the formation of hydrogen bonds with other electronegative atoms, such as N, attached to polymer chains[11]. This shift has not been observed in our hydrogels. A smaller shift is observed for sample 5.

Three or even sometimes four different peaks are observed to be associated with the symmetric stretch vibrations of the P–O–(R) band and the presence of various ionic phosphate groups, e.g. as HPO_4^{2-} or $H_2PO_4^-$ (see samples 13, 14, 17 and 18 in *Table 2*). Values of the frequencies of the peak positions are listed in *Table 2* where these bands have been assigned according to previously published data[10–13]. The presence of both HPO_4^{2-} and $H_2PO_4^-$ moieties implies that the transport of protons may occur via a Grotthus type mechanism, which involves an exchange of protons between a Bronsted type acid ($H_2PO_4^-$) and a Bronsted type base (HPO_4^{2-}). The strong P–O–(R) stretching band observed at 1001 cm^{-1} for pure H_3PO_4 shifts to a lower frequency range after complexation with polymer chains. A larger shift to 961 cm^{-1} is observed for acid/AAM molar ratios higher than 1.6 : 1 (see samples 17 and 18 in *Table 2*). For these two samples the HPO_4^{2-} band appearing at 890–875 cm^{-1}, as for the other samples, is not observed although an additional band at 1060 cm^{-1} is observed, which, on the basis of literature data[10–13], has been attributed to the presence of $H_2PO_4^-$ moieties. This band is not observed for samples of lower H_3PO_4 concentrations. The presence of this band can be explained by the self-ionization of an excess of H_3PO_4. The presence of HPO_4^{2-} moieties is either masked by the stronger $H_2PO_4^-$ peak or the concentration of HPO_4^{2-} in these samples is much lower than that of $H_2PO_4^-$ due to the lower dissociation constant for the second step of H_3PO_4 dissociation. This behaviour suggests that H_3PO_4 participates in the reaction with polymer chains, which results in the weakening of the P–O–(R) bonds. On the other hand, in samples 17 and 18 there is an excess of free H_3PO_4, which dissociates, giving solvated H_3O^+ ions and $H_2PO_4^-$ moieties, and hence there is an increase in

Table 2 Position of the maxima of the *FT* i.r. bands measured for H_3PO_4 doped hydrogel protonic electrolytes

Sample code	Acid/AAM ratio	P=O band (cm^{-1})	P–O–R band (cm^{-1})	HPO_4^{2-} (cm^{-1})	$H_2PO_4^-$ (cm^{-1})
1[a]	1.6/1		988	887	1136
2[a]	1.6/1		988	883	1117
3[a]	1.6/1		975	888	1115
4[a]	1.6/1	1260	969	883	1107
5[a]	1.6/1	1243	958	885	1120
12[b,c]	1.6/1		994	885	1121
13[b,d]	1.6/1				1120, 1070
14[b,e]	1.6/1				1121, 1071
15[b]	1.2/1	1260	988	877	1121
16[b]	1.4/1		990	880	1124
17[b]	1.8/1	1260	961		1130, 1060
18[b]	2.0/1	1260	961		1134, 1061
H_3PO_4		1260	1001	890	1133

[a] For sample compositions see *Table 1*
[b] Samples of the same AAM, MBAA and agar concentration as sample 1
[c] Sample containing 15 wt% of water
[d] Sample containing 30 wt% of water
[e] Sample containing 40 wt% of water
The concentration of water in other samples is equal to 20 wt%

Table 3 Position of the maxima of the *FT* i.r. bands measured for H_2SO_4 doped hydrogel protonic electrolytes

Sample code	Frequency (cm^{-1})	Frequency (cm^{-1})	Frequency (cm^{-1})
6	1178	1052	869
7	1181	1052	873
8	1174	1049	870
9	1176	1049	871
10	1174	1047	873
11	1175	1052	867

conductivity for acid/AAM molar ratios higher than 1.6:1. The presence of excess of H_3PO_4 has been confirmed by the d.s.c. data in which the intensity of the H_3PO_4 endothermic transition occurring at 130–140°C increases with an increase in the concentration of H_3PO_4.

A shifting down in frequency of the maximum in the P–O–(R) band is also observed when the concentration of MBAA (cross-linking agent) increases. (Compare samples 1 with 4 and 5 in *Table 2*.) The decrease in frequency could be associated with a weakening of the P–O–R bonds due to a stronger bonding of H_3PO_4 with the highly cross-linked stiff polymer chains.

An increase in the water concentration results in the appearance of the free $H_2O_4^-$ band at approximately 1070 cm^{-1}, probably due to easier dissociation of H_3PO_4 occurring in the interstitial water phase. This confirms that, for water concentrations higher than 30 wt%, the conductivity occurs via conducting pathways formed by interstitial water. Similar mechanisms have been postulated on the basis of the temperature dependence of the conductivity described above.

FT*i.r. studies of H_2SO_4 doped hydrogel electrolytes*

Similar to those of H_3PO_4 doped hydrogels the symmetric stretch N–H vibrations of protonated NH_3^+ and unprotonated NH_2 amide groups are difficult to analyse quantitatively. However, the presence of both NH_3^+ and NH_2 groups is confirmed on the basis of the *FT*i.r. spectra. Vibrations characteristic of moieties containing sulfur occur in the frequency range 1300–600 cm^{-1}. The most important of them are[14,15]:

SO_4^{2-} : 1130–1080 cm^{-1} (vs); 680–610 cm^{-1} (mw)

HSO_4^- : 1180–1160 cm^{-1} (s);
1080–1000 cm^{-1} (s); 880–840 cm^{-1} (s)

The maxima of the *FT* i.r. bands measured for these hydrogel electrolytes are summarized in *Table 3*. There is no evidence for the presence of free SO_4^{2-} anions for all of the protonic electrolytes studied. All three frequencies listed in *Table 3* can be attributed to the presence of HSO_4^- anions. These observations show that H_2SO_4 is mostly involved in the protonation of the NH_2 amide groups and possibly in the protonation of the carbonyl oxygen groups in the poly(acrylamide) chains. H_2SO_4 could also be involved in the cross-linking of polymer chains by forming hydrogen bonds with the oxygen or nitrogen atoms in the polymer chains. Cross-linking via a reaction of H_2SO_4 with amide double bonds during the polymerization cannot be excluded for samples of a high H_2SO_4 concentration. The transport of protons can occur via exchange of protons between protonated and unprotonated amide groups. The exchange of protons between NH_3^+ and HSO_4^+ groups is also possible. Protonated carbonyl groups can also be involved in ionic transport. On the basis of the *FT*i.r. results the presence of HSO_4^-/SO_4^{2-} acid/base pairs can be excluded. Therefore, the possibility of a Grotthus type proton conduction mechanism is less probable than in the case of the H_3PO_4 hydrogels.

Thermal stability studies of H_3PO_4 doped hydrogel electrolytes

In this section the reproducibility of the ionic conductivity of hydrogels doped with H_3PO_4 at annealing temperatures of 70, 80 and 100°C is examined. In our experiments, conductivities of hydrogel protonic electrolytes

were studied over a long period of time using impedance spectroscopy. Gel samples were sandwiched between two stainless steel blocking electrodes and placed in a temperature controlled oven. The samples were annealed at these temperatures for approximately 6–8 h and conductivity measurements were taken every hour. If the conductivity measured during this period remained at 80–90% of the initial conductivity, σ_{in}, the impedance experiments were continued for a longer period (up to 30 h). Electrolytes characterized by H_3PO_4/AAM molar ratios equal to 1.2/1, 1.6/1 and 2.0/1 were used in our investigations.

Figure 5 presents the changes in the conductivity measured at 100°C with time for samples of H_3PO_4/AAM molar ratios equal to 1.2/1, 1.6/1 and 2.0/1. The conductivity changes are illustrated as the ratio of the conductivity σ (as measured during the annealing) divided by σ_{in}. The conductivities measured for all samples decrease with time. The decrease in conductivity measured for the sample of the lowest H_3PO_4 concentration is higher than for the other samples studied. For the samples of H_3PO_4/AAM ratio equal to 1.6/1 and 2.0/1 the σ/σ_{in} ratio is still over 0.75 after the first hour of annealing at 100°C. A considerable drop in the conductivity of these samples is measured between the first and second hours of annealing. After 4 h of annealing, conductivities decreased to 0.2–0.3 of σ_{in} and then further slightly decreased during continued annealing. For the sample containing the lowest amount of H_3PO_4 an abrupt decrease in the conductivity is already apparent after the first half hour of annealing. After 4 h of annealing the conductivity measured for this latter sample is approximately two orders of magnitude lower than σ_{in}.

In *Figure 6* changes in the conductivity measured at 80°C with time are depicted for all of the samples studied. The decrease in the conductivity is much smaller than that measured at 100°C (cf. *Figures 5* and *6*). Conductivities measured after 6 h of annealing for samples of H_3PO_4/AAM = 1.2/1 and H_3PO_4/AAM = 1.6/1 are within 40–50% of σ_{in}. For the H_3PO_4/AAM = 2.0/1 sample, conductivity decreases to approximately 80–85% of σ_{in} during the first 2 h of annealing and than remains almost unchanged. The long-term experiments performed for this sample for over 30 h showed a small gradual decrease in conductivity down to 60–70% of σ_{in}. The final conductivities are, however, still above 5×10^{-3} S cm^{-1}.

Figure 7 presents changes in the conductivities measured at 70°C for all of the samples studied. The trends observed are similar to those shown in *Figure 6*. The final conductivities measured after 6 h of annealing of the H_3PO_4/AAM = 1.2/1 or 1.6/1 samples are within 60–70% of the σ_{in}. The conductivity measured for the electrolytes of the H_3PO_4/AAM ratio 2.0/1 remains in the range 90–95% of σ_{in}. A further 10% decrease in the conductivity of σ_{in} is measured during further annealing of this sample from 10 to 30 h.

The results of these experiments show that the conductivity of hydrogels doped with H_3PO_4 decreases with time during measurements carried out at 100, 80 and 70°C. The decrease observed at 100°C is the most

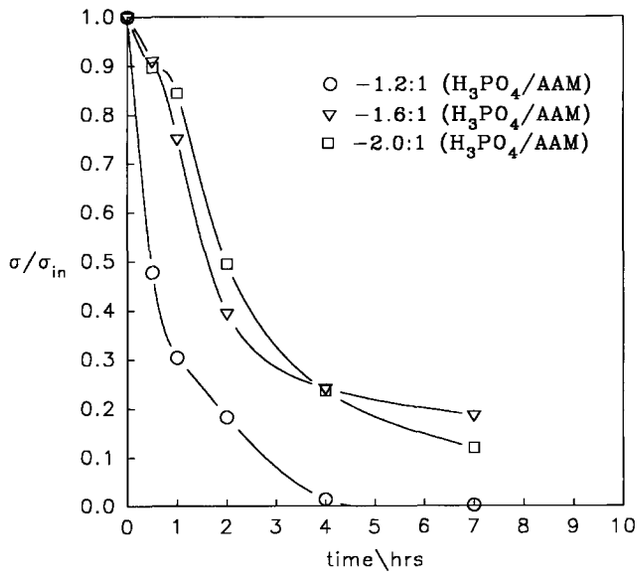

Figure 5 Changes of the σ/σ_{in} ratio with time at 100°C

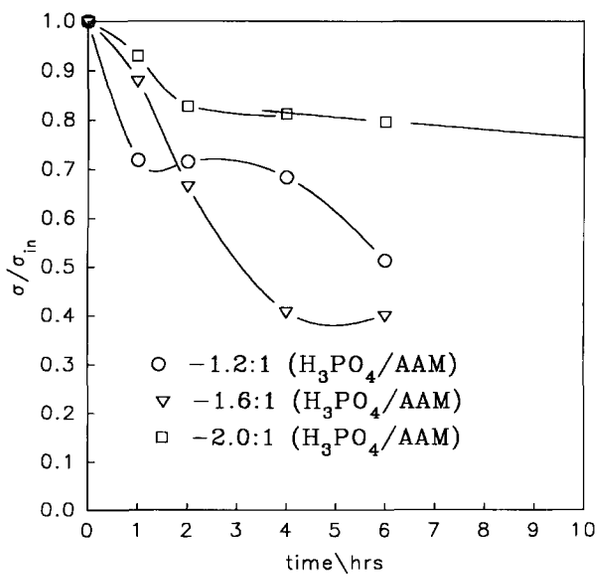

Figure 6 Changes of the σ/σ_{in} ratio with time at 80°C

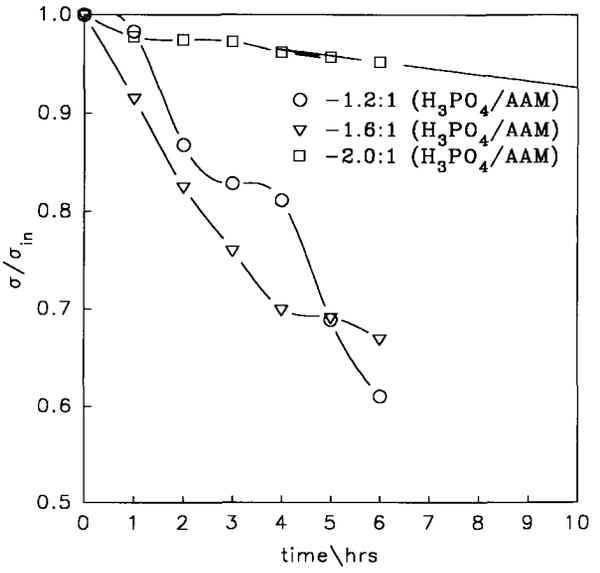

Figure 7 Changes of the σ/σ_{in} ratio with time at 70°C

Table 4 Conductivity parameters calculated on the basis of VTF [equation (2)] or Arrhenius [equation (1)] semi-empirical forms and used after for EMT calculations [equation (3)]

Phase type	A(S K$^{0.5}$ cm^{-1})	Bk_B^{-1} (K)	T_σ (K)	σ_0 (S cm^{-1})	E_a (eV)
PAAM/H_3PO_4 dry electrolyte	6.5	548	174		
Aqueous H_3PO_4 electrolyte				12.78	0.15

significant. It has also been noticed that the decrease observed for the sample containing the highest concentration of H_3PO_4 is much smaller (particularly at 80 and 70°C) than for the other samples. The decrease in the conductivity observed is most probably due to drying of the sample and loss of the excess of water at relatively high temperatures. The smaller decreases in conductivity observed at 70 and 80°C seem to confirm this hypothesis. It should be stressed that samples were not moisturized during the impedance experiments. Therefore, after long periods of time, hydrogel samples become similar to the 'dry' PAAM/H_3PO_4 electrolytes[2,3]. The highest stability of the conductivity measured for hydrogels with the highest H_3PO_4 concentration can be explained on the basis of the results obtained by Połtarzewski and Przyłuski for similar hydrogel systems[16]. These authors demonstrated that the absorption of water by hydrogels decreases with an increase in the H_3PO_4/AAM molar ratio and for H_3PO_4/AAM = 2 is five times lower than for the hydrogel of the H_3PO_4/AAM = 1.2 and three times lower than for the hydrogel of the H_3PO_4/AAM = 1.6. This implies that the conductivity of the sample with the highest H_3PO_4 concentration is less dependent on the content of water; this is in agreement with the above observations.

CONDUCTION MECHANISM IN HYDROGELS—EMT APPROACH

As demonstrated above (see *Figure 2*) the conductivity of hydrogel electrolyte increases with an increase in water concentration. Therefore, we assume that our hydrogel is a mixture of two phases. These are a 'dry' PAAM/acid phase with no water present and a water/acid phase trapped in a polymer phase. The bulk conductivity of hydrogels is a result of interactions between these two phases. Therefore, it seems to be reasonable to apply an EMT to describe the conductivity *versus* water concentration isotherm presented in *Figure 2*. To make these calculations easier we have assumed that each of the phases mentioned above has spherical symmetry. Under these assumptions each phase in the heterogenous gel material is symmetrically embedded in a self-consistent effective medium with the same effective conductivity σ^* as the bulk hydrogel electrolyte. Our description is thus given in terms of the complex conductivity of this inhomogeneous dielectric material considered to possess macroscopic uniformity. The general self-consistent equation for the multiphase material is[17–19]

$$\sum_i w_i \frac{\sigma_i - \sigma^*}{\sigma_i + (d-1)\sigma^*} = 0 \qquad (4)$$

Here, d is a dimensionality parameter equal to 3 for spherical aggregates, σ_i $(i = 1, 2)$ are conductivities of the water phase (σ_1) or 'dry' polymer phase (σ_2) and w_i is the volume fraction of the ith phase. All EMT calculations described below are based on equation (4).

In order to perform EMT calculations the temperature dependence for conductivity for the 'dry' PAAM/H_3PO_4 (H_3PO_4/PAAM = 1.6) system and for an aqueous electrolyte of H_3PO_4 (of the same acid concentration as for hydrogels with [H_3PO_4]/AAM = 1.6) were experimentally determined. The temperature dependence of conductivity for the 'dry' PAAM/H_3PO_4 electrolyte can be fitted by the VTF type equation [equation (2)] whereas the Arrhenius form [equation (1)] was used for the description of the conductivity of the aqueous electrolyte. The parameters found from these fittings are summarized in *Table 4*. These parameters have been used in the EMT calculations.

As can be seen from *Figure 2* the EMT model fits the experimental data quite well. We have also modelled the temperature dependence of conductivity for hydrogel electrolytes of various water concentrations using an EMT approach. For samples with water concentrations below 30 vol% a curvature of the conductivity *versus* reciprocal temperature plots is observed. This curvature can still be recognized for samples containing 41 vol% of water. For water concentrations higher than 45 vol% on Arrhenius behaviour for the temperature dependence of the conductivity is observed. The model data presented are in good agreement with the experimental observations, indicating that ionic transport preferably occurs in the aqueous phase. For samples in which the water concentration is above the percolation threshold, conducting pathways via interstitial water are achieved. This is manifested in a considerable enhancement in conductivity in a comparison with the 'dry' PAAM/H_3PO_4 system.

CONCLUSIONS

Studies on PAAM based hydrogels doped with H_3PO_4 and H_2SO_4 have been performed. A reproducible method for the preparation of these has been achieved and protonic conductivities have been obtained in the range 10^{-3}–10^{-2} S cm^{-1} at ambient temperatures for an aqueous AAM/MBAA network doped with strong acid. These conductivities increase to 10^{-1} S cm^{-1} at around 100°C. The highest conductivities were obtained for an acid/AAM molar ratio equal to 2/1 and water concentrations higher than 45 vol%; these were about 3×10^{-2} S cm^{-1} at room temperature. These highest conductivities are dependent on maintaining a high water content whereas in the water concentration range between 25 and 45 vol% quite stable protonic conduction at $\sim 1 \times 10^{-2}$ S cm^{-1} is found at room temperature. Long-term conductivity studies of H_3PO_4 doped hydrogels in the temperature range 70–100°C indicate 'drying' of these hydrogels and a decrease in conductivity. This decrease is more pronounced for samples with low acid concentrations. Nevertheless, the ionic conductivity for these hydrogels with a H_3PO_4/AAM molar ratio of 2/1 remains almost unchanged with time for temperatures up to 70°C. The variation of ionic conductivity with

temperature in these hydrogels for water concentrations <45 vol% is VTF and for water concentrations >45 vol% is Arrhenius. It is suggested that hydrogel electrolytes can be treated within an EMT model as a two-component mixture of a 'dry' PAAM/acid electrolyte and an aqueous solution of a strong acid. Such a model fits the experimental conductivity data well.

D.s.c. and *FT* i.r. studies of these hydrogels have been made to provide information on the ionic conduction mechanisms involved. No first-order transitions are observed for the H_3PO_4 doped hydrogels for temperatures lower than 100°C. Values of T_g are a function of the water concentration (plasticization) and increase as the water concentration decreases; T_g also increases with an increase in the concentration of MBAA and decreases with increase in the agar concentration, which, acting as a gelation agent, absorbs water which in turn plasticizes the gel. H_2SO_4 doped hydrogel electrolytes decompose at temperatures higher than 70°C; H_3PO_4 doped hydrogels are stable above 100°C.

FT i.r. spectra confirm that both protonated and unprotonated NH_2 amide groups coexist for all of the samples studied, implying that the transport of protons could occur via proton exchange between these two amide groups. Also, *FT* i.r. spectra confirm the presence of both $H_2PO_4^-$ and HPO_4^{2-} moieties so that the transport of protons may occur via a Grotthus type mechanism involving an exchange of protons between a Bronsted type acid ($H_2PO_4^-$) and a Bronsted type base (HPO_4^{2-}). For the H_2SO_4 doped hydrogels the presence of both NH_3^+ and BH_2 groups is confirmed by *FT* i.r. These observations show that H_2SO_4 is mostly involved in the protonation of the NH_2 amide groups and possibility in the protonation of the carbonyl oxygen groups. The transport of protons can occur via exchange of protons involving the amide and carbonyl groups. Since *FT* i.r. does not indicate the presence of HSO_4^-/SO_4^{2-} acid/base pairs the possibility of a Grotthus type conduction mechanism has a low probability.

ACKNOWLEDGEMENT

This work was financially supported by British Gas.

REFERENCES

1 Scrosati, B. 'Applications of Electroactive Polymers', Chapman and Hall, London, 1994
2 Lassegues, J. C. in 'Proton Conductors: Solids, Membranes and Gel—Materials and Devices' (Ed. P. Colomban), Cambridge University Press, Cambridge, 1992, Ch. 20
3 Lassegues, J. C., Desbat, B., Trinquet, O., Cruegge, F. and Poinsignon, C. *Solid State Ionics* 1989, **35**, 17
4 Daniel, M. F., Desbat, B., Cruegge, F., Trinquet, O. and Lassegues, J. C. *Solid State Ionics* 1988, **28–30**, 637
5 Donoso, P., Gorecki, W., Berthier, C., Defendini, F., Poinsignon, C. and Armand, M.B. *Solid State Ionics* 1988, **28–30**, 969
6 German Patent No. 27 252 261, 1978
7 Łukaszczyk, J., Kuc, A., Lorenc, J. and Pradellok, W. *Appl. Chem. (Chemica Stosowana)* 1990, **XXXIV**, 1 (English edition)
8 Wieczorek, W., Florjańczyk, Z. and Stevens, J. R. *Electrochim. Acta* 1995, **40**, 2327
9 Wieczorek, W., Dąbrowska, A., Florjańczyk, Z. and Stevens, J. R. in 'Proceedings of First International Symposium on New Materials for Fuel Cell Systems' (Ed. O. Savadogo), Les Editions École Polytechnique Montréal, Montreal, 1995
10 Takahashi, T., Tanase, S., Yamamoto, O. and Yamaguchi, S. *J. Solid State Chem.* 1976, **17**, 353
11 Bellamy, L. J. in 'Infra-red Spectra of Complex Molecules', Chapman and Hall, London, 1975, Ch. 18
12 Thomas, G. and Chittenden, H. *Spectrochim. Acta* 1964, **20**, 467
13 Tanaka, R., Yamamoto, H., Kawamura, S. and Iwase, T. *Electrochim. Acta* 1995, **40**, 2422
14 Bellamy, L. J. in 'Infra-red Spectra of Complex Molecules', Chapman and Hall, London, 1975, Chs 21 and 22
15 Rao, C. N. R. in 'Chemical Applications of Infra-Red Spectroscopy', Academic Press, New York and London, 1963, Ch. 7
16 Połtarzewski, Z. and Przyłuski, J. in 'Proceedings of First International Symp on New Materials for Fuel Cell Systems', (Ed. O. Savadogo), Les Editions École Polytechnique Montréal, Montreal, 1995
17 Nan, C. W. *Progr. Mater. Sci.* 1993, **37**, 1
18 Such, K., Stevens, J. R., Wieczorek, W., Siekierski, M. and Florjańczyk, Z. *J. Polym. Sci., Polym. Phys. Edn* 1994, **32**, 2221
19 Van Heumen, J., Wieczorek, W., Siekierski, M. and Stevens, J. R. *J. Phys. Chem.* 1995, **99**, 15142